Fermilab
FERMILAB-Pub-04/007-A January 2004

ANGULAR CORRELATIONS OF THE MEV COSMIC GAMMA RAY BACKGROUND

Pengjie Zhang and John F. Beacom
NASA/Fermilab Astrophysics Center, Fermi National Accelerator Laboratory, Batavia, IL 60510-0500

January 17, 2004

ABSTRACT

The measured cosmic gamma ray background (CGB) spectrum at MeV energies is in reasonable agreement with the predicted contribution from type Ia supernovae (SNIa). But the characteristic features in the SNIa gamma ray spectrum, weakened by integration over source redshifts, are hard to measure, and additionally the contributions from other sources in the MeV range are uncertain, so that the SNIa origin of the MeV CGB remains unproven. We show that since different CGB sources have different clustering properties and redshift distributions, by combining the CGB spectrum and angular correlation measurements, the contributions to the CGB can be identified and separated. The SNIa CGB large-scale structure follows that of galaxies. Its rms fluctuation at degree scales has a characteristic energy dependence, ranging from $\sim 1\%$ to order of unity and can be measured to several percent precision by proposed future satellites such as the Advanced Compton Telescope. With the identification of the SNIa contribution, the SNIa rate could be measured unambiguously as a function of redshift up to $z \sim 1$, by combining both the spectrum and angular correlation measurements, yielding new constraints on the star formation rate to even higher redshifts. Finally, we show that the gamma ray and neutrino backgrounds from supernovae should be closely connected, allowing an important consistency test from the measured data. Identification of the astrophysical contributions to the CGB would allow much greater sensitivity to an isotropic high-redshift CGB contribution arising in extra dimension or dark matter models.

Subject headings: cosmology: large scale structure; gamma rays: theory–diffuse background; star: formation

1. INTRODUCTION

Type Ia supernovae (SNIa) produce intense fluxes of nuclear gamma rays, following the electron-capture decays of ^{56}Ni and ^{56}Co, contributing significantly to the MeV cosmic gamma ray background (CGB). The predicted spectrum shape and normalization are both in reasonable agreement with CGB measurements from COMPTEL (Weidenspointner 1999) and SMM (Watanabe, Leising, Share, & Kinzer 2000). The case for the SNIa origin of the MeV CGB, including other possible sources, and the dependence on cosmological parameters and the star formation rate, has been nicely summarized by Watanabe, Hartmann, Leising, & The (1999) and Ruiz-Lapuente, Cassé & Vangioni-Flam (2001).

The SNIa gamma ray spectrum has strong line features around 1 MeV, and integration over SNIa redshifts turns these into a series of steps (Clayton & Silk 1969; Clayton & Ward 1975; The, Leising, & Clayton 1993). But these characteristic spectral features are below the resolution of existing measurements, and so the SNIa origin of the MeV CGB remains unproven. More fundamentally, combinations of several proposed contributions to the MeV CGB may also produce a spectrum in reasonable agreement with observations. Since redshift information is mixed when integrating over sources, this potential degeneracy makes identification of the CGB sources challenging.

We propose new techniques to identify the origin of the MeV CGB, based on the observation that angular correlations of the CGB will reveal crucial information on the three-dimensional source distributions. Since SNIa are associated with galaxies, the SNIa CGB should follow the galaxy distribution. Other possible MeV CGB sources, such as MeV blazars (Blom et al. 1995) and cosmic ray shock acceleration (Miniati 2003), have different clustering and redshift distributions, and would lead to different angular correlations in the CGB. Thus CGB angular correlations can be exploited to break degeneracies that are present if only the spectrum is used. More importantly, the line emission features of the SNIa CGB are strongly enhanced in the autocorrelation function, allowing unambiguous identification of the SNIa contribution to the CGB. Furthermore, by cross correlating the CGB with galaxies, important redshift information can be recovered. The correlated angular fluctuations in the CGB that we consider are intrinsically different from the uncorrelated Poisson fluctuations considered by Cline & Gao (1990) and Gao, Cline, & Stecker (1990); that case is appropriate if there are very few sources or detected photons per angular bin, which is not the case here. Sources like MeV blazars, being rare, and also exhibiting strong variability (Zhang et al. 2002), will lead to uncorrelated angular fluctuations.

Such unambiguous extraction of SNIa CGB allows a statistically robust measure of the supernova rate (SNR) and its evolution and hence also the star formation rate (SFR). A routine one year CGB survey would reflect the statistics of $\sim 10^7$ unresolved SNIa, with little obscuration by dust. In contrast, individual SNIa seen by gamma ray telescopes are expected to be very rare (Timmes & Woosley 1997). Even the proposed SNAP satellite would only optically resolve ~ 1000 SNIa per year.

We use the SNIa contribution to the CGB to illustrate

Electronic address: zhangpj@fnal.gov, beacom@fnal.gov

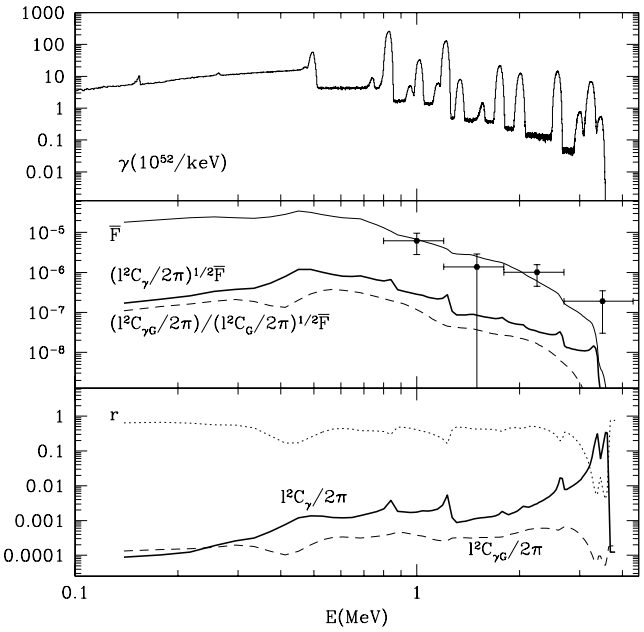

FIG. 1.— SNIa spectrum, CGB mean flux spectrum $\bar{F}$ (in units of photons cm^{-2} s^{-1} sr^{-1} keV^{-1}), angular power spectrum C_γ, and cross correlation power spectrum $C_{\gamma G}$ with galaxies. C_γ and $C_{\gamma G}$ are represented in two ways. Both scale as $\ell^{-1.3}$ and are evaluated at $\ell = 100$. The CGB-galaxy cross correlation coefficient r is also shown. Emission line features are smoothed out in $\bar{F}(E)$ and $C_{\gamma G}$ by integration over SNIa redshifts but survive in C_γ because the auto correlation amplifies these line features. The large amplitude of C_γ at high E reflects strong CGB correlations at small scales and low redshifts. For the same reason, the CGB and galaxies have different redshift contributions, causing a decrement in $C_{\gamma G}$ and r.

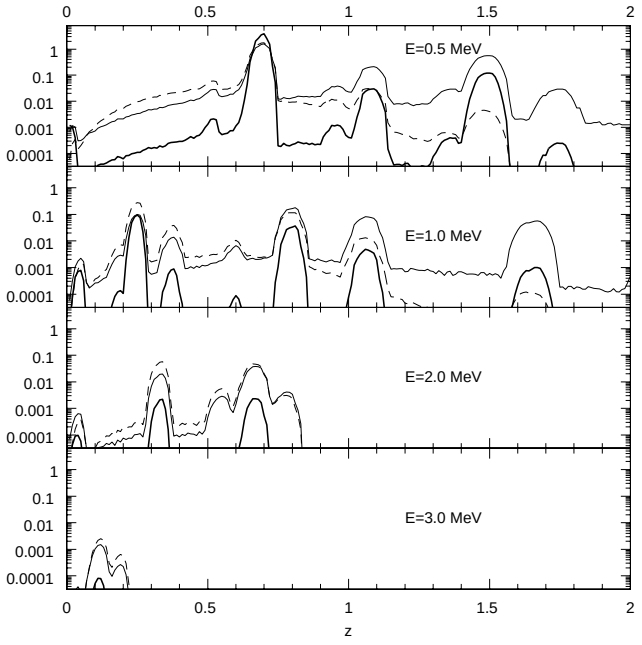

FIG. 2.— Logarithmic contributions to $\bar{F}_n$ (thin solid lines), $C_\gamma \bar{F}_n^2$ (thick solid lines) and $C_{\gamma G}\bar{F}_n\bar{\Sigma}_G$ (dashed lines) from different z for the displayed energy values. These are dominated by line emissions in a series of redshift ranges, which allows inversion for the SNR. It also shows that $C_{\gamma G}$ can be best measured by choosing the redshift interval in the galaxy survey to best overlap the most significant SNIa redshift range.

our proposed techniques. We calculate the SNIa CGB mean flux spectrum in §2, the SNIa CGB auto correlation in §3, and the cross correlation with galaxies in §4, discussing the observational feasibility in §5. Based on the measurements of flux spectrum, auto correlation, and cross correlation with galaxies, respectively, we present three new and independent methods to directly measure the SNR. Finally, we discuss the impact of improved sensitivity to new physics contributions to the CGB.

2. CGB MEAN FLUX SPECTRUM

The mean number flux spectrum of the SNIa CGB is

$$\bar{F}(E) = \int \left[\frac{L(E(1+z),z)}{4\pi} R_{\rm SN}(z)\right] d\chi\,, \qquad (1)$$

where $L(E)$ is the average number of gamma rays per SNIa per energy interval, $R_{\rm SN}(z)$ is the SNR, and χ is the comoving distance (we assume $\Omega_m = 0.3$, $\Omega_\Lambda = 1-\Omega_m$, and $h = 0.7$). Since $L(E)$ is well-predicted, $\bar{F}(E)$ can be used to constrain the SFR (Watanabe, Hartmann, Leising, & The 1999; Ruiz-Lapuente, Cassé & Vangioni-Flam 2001). The SNIa spectrum, adopted from Fig. 3a of Ruiz-Lapuente, Cassé & Vangioni-Flam (2001), is shown in the top panel of Fig. 1. The resulting mean flux spectrum, shown in the middle panel of Fig. 1, is sufficient to account for both the shape and normalization of the COMPTEL (Weidenspointner 1999) and (not shown) SMM (Watanabe, Leising, Share, & Kinzer 2000) data over the energy range $0.5 \lesssim E \lesssim 3$ MeV. At lower or higher energies, other sources besides SNIa are required to reproduce the observations.

The SNR is determined by the SFR, the efficiency for producing SNIa, and the characteristic time scale $t_{\rm SN}$ for a binary system to produce a SNIa. We assume that every $900 M_\odot$ of stellar mass turns into a SNIa and $t_{\rm SN} = 1$ Gyr for a white dwarf + non-white-dwarf system (Ruiz-Lapuente, Cassé & Vangioni-Flam 2001). For the SFR, we adopt (Hippelein et al. 2003) $R_{SF}(z \le 1.2) = 10^{-2.1}\exp(t/2.6\,{\rm Gyr})$ and $R_{SF}(z > 1.2) = R_{SF}(1.2)\exp\left(-(t-t(z=1.2))/2.5\,{\rm Gyr}\right)$, both in units of $M_\odot$ yr^{-1} Mpc^{-3}, and where t is the look-back time.

Past efforts of analyzing the mean flux spectrum can be improved by an inversion method. The spectrum can be discretized as matrix product,

$$\bar{\mathbf{F}} = \mathbf{K}\cdot\mathbf{R_{SN}}\,, \qquad (2)$$

where the components of $\bar{\mathbf{F}}$ and $\mathbf{R_{SN}}$ are $\bar{F}(E_i)$ and $R_{SN}(z_j)$, and kernel matrix $\mathbf{K}$ is specified by

$$\mathbf{K}_{ij} = \frac{d\chi/dz|_{z_j}}{4\pi}\int_{z_j-\Delta z_j/2}^{z_j+\Delta z_j/2} L_n(E_i(1+z),z)\,dz\,. \qquad (3)$$

Due to strong variations in $L_n(E)$, we must use integral form instead of evaluating it at the median z_j.

We split L into a smooth part L^S and a line emission part L^L. The line emission part L^L can be approximated as a sum of delta-like functions, $\sum L^L_m(E,E^L_m)$. The central values E^L_m do not change with z, but $L^L_m(E,E^L_m)$ may depend on z due to metallicity and environment evolu-

tion. For simplicity, we neglect this possible redshift dependence, which can in principle be calibrated by SNIa observations in other bands. Thus

$$\mathbf{K}_{ij} \simeq \frac{d\chi/dz|_{z_j}}{4\pi}\left[L^S(E_i(1+z_j),z_j)\Delta z_j + \sum_m \frac{g_m(z_j)}{E_i}\right], \quad (4)$$

where $g_m(z) = \int_0^\infty L_m^L(E',z)\,dE'$ is the total number flux from the E_m^L emission line at z, and the values m are determined by $E_m^L/E - 1 \in (z_j - \Delta z_j/2, z_j + \Delta z_j/2)$. In the relevant range, $\bar{F}(E)$ is dominated by the line emissions, and the smooth part (L^S) can be neglected in Eq. (4).

For each E, at most several specific emission lines and hence relatively narrow ranges of redshift contribute, as shown in Fig. 2. Since these peaks are narrow in redshift space, $\Delta z_j = 0.1$ is sufficient to minimize edge effects. It is sufficient to only keep the first several dominant g_m, so that $\mathbf{K}$ reduces to a sparse matrix. This keeps the dominant signal while minimizing noise from other z ranges, simplifying and stabilizing the inversion. While present data are not yet sufficient, this method of inversion from $\bar{F}(E)$ can be used to measure the SNR up to $z \sim 1.5$, as shown in Fig. 2.

3. CGB ANGULAR AUTOCORRELATION

The CGB angular autocorrelation has a different dependence on the SNR and provides a new method to measure it. Since SNIa appear in all galaxy types, we expect the that the SNR follows the galaxy distribution with a constant bias b after averaging over a sufficient number of galaxies. Additionally, since only SNIa produce the characteristic spectral features, the bias could be measured. For simplicity, we assume $b = 1$ throughout this paper. The angular resolution of the CGB experiments is generally $\sim 1^\circ$, and at these scales we expect Gaussian fluctuations in the CGB. Since a $(1^\circ)^2$ patch of sky contains $\sim 10^5$ galaxies, the constant bias assumption should hold very well. In large field of view CGB telescopes such as COMPTEL, each $(1^\circ)^2$ angular bin receives gamma rays from $\sim 10^3$ SNIa. Thus there should be no bias originating from the time variation caused by the finite duration of the SNIa (~ 1 year), and the possible dispersion in individual SNIa emission spectra is also well averaged. Then $F(E)$ is given by

$$\bar{F}(E) = \int \left[\frac{L(E(1+z),z)}{4\pi} R_{SN}(z)\right](1+\delta_G)\,d\chi\,, \quad (5)$$

where δ_G is the relative galaxy number density fluctuation.

The widths of emission lines are generally several percent of the peak energies (see Fig. 1), corresponding to spatial separations of several 30 Mpc/h. Since these are much larger than the galaxy-galaxy correlation length, we can use Limber's equation (Peacock 1999) in the relevant multipole range ($\ell \gtrsim 10$ or $\theta \lesssim 30^\circ$) to obtain C_γ:

$$\frac{\ell^2}{2\pi}C_\gamma(\ell)\bar{F}^2 = \int \left[L(E(1+z),z)\frac{R_{\rm SN}(z)}{4\pi}\right]^2 \pi\frac{\chi}{\ell}\Delta_G^2(\frac{\ell}{\chi},z)d\chi$$
$$\simeq \sum_m \left(\frac{R_{SN}(z_j)}{4\pi}\right)^2 \frac{g_{2,m}(z_j)}{E}$$
$$\times\, \pi\frac{\chi(z_j)}{\ell}\Delta_G^2(\frac{\ell}{\chi},z_j)\frac{d\chi}{dz}|_{z_j}\,. \quad (6)$$

Due to the amplification in the square, only the line emission features in L need to be considered, and $g_{2,m}$ is defined analogously to g_m above, except for $L^2(E,z)$ instead of $L(E,z)$. Since both the galaxy power spectrum (variance) Δ_G^2 and $C_\gamma\bar{F}^2$ are observables, by the inversion methods discussed in §2, Eq. (6) can be applied to obtain $R_{SN}(z)$. Since L^2 is much sharper than L, the kernel matrix is more sparse than that of $\bar{F}$, so that different E ranges are less correlated, improving the error and the stability of the inversion.

To quantify the sparse feature of this kernel matrix, we calculate the contributions to C_γ from various z. Here Δ_G^2 can be calculated from galaxy correlation function, which we assume to be $\xi_G(r,z) = D^2(z)(r/[5\ {\rm Mpc}/h])^\alpha$, with $\alpha = -1.7$, as inferred from the SDSS angular correlation results (Connolly et al. 2002), and where $D(z)$ is the linear density growth factor. These assumptions are accurate enough to illustrate our main results.

A direct prediction is then $C_\gamma(\ell) \propto C_G(\ell) \propto \ell^{-\alpha-3} = \ell^{-1.3}$. As expected, C_γ shows strong signatures of the emission lines, as shown in Fig. 1. There are only several important E_m^L (Fig. 2), so the inversion is straightforward. For example, a measurement at 0.5 MeV would directly measure $R_{SN}(z)$ at $z = 0.7$. Since the density fluctuations weaken toward high z, C_γ is mainly sensitive to measuring $R_{SN}(z)$ for $z \lesssim 1$.

4. CGB-GALAXY ANGULAR CROSS CORRELATION

Since the SNIa CGB is tightly correlated with galaxies, by using the galaxy clustering data as a function of photometric redshift range, the SNIa redshift distribution can be recovered. This cross correlation provides a new and robust way to identify CGB sources. For example, any CGB sources at high redshifts have no correlation with galaxies, which is particularly important for testing some new physics models, discussed further below. Furthermore, the cross correlation provides another way to measure the SNR. The cross correlation power spectrum $C_{\gamma G}$ with galaxies in the redshift range $[z_1, z_2]$ is

$$\frac{\ell^2}{2\pi}C_{\gamma G}(\ell)\bar{F}\bar{\Sigma}_G = \int_{z_1}^{z_2}\left[\frac{L(E(1+z),z)}{4\pi}R_{SN}(z)\right]$$
$$\times\, \pi\frac{\chi}{\ell}\Delta_G^2(\frac{\ell}{\chi},z)\frac{dn}{dz}dz\,, \quad (7)$$

where $n(z)$ is the galaxy number distribution function and the galaxy surface density is defined as $\Sigma_G = \int dn/dz(1+\delta_G)dz$. We adopt $dn/dz = 3z^2/2/(z_m/1.412)^3\exp(-(1.412z/z_m)^{1.5})$ and choose the median redshift $z_m = 0.5$ for SDSS (Dodelson et al. 2002).

Just as for $\bar{F}$ and C_γ, the contribution at a given energy is dominated by at most several redshift bins, as shown in Fig. 2, due to the SNIa line emission features. These redshift bins are then optimal for the cross correlation measurement because they contain the strongest signal. In this limit, Eq. (7) becomes

$$\frac{\ell^2}{2\pi}C_{\gamma G}(\ell)\bar{F}\bar{\Sigma}_G \simeq \frac{R_{SN}(z_j)}{4\pi}\frac{dn}{dz}|_{z_j}\frac{g_m(z_j)}{E}$$
$$\times\, \pi\frac{\chi(z_j)}{\ell}\Delta_G^2(\frac{\ell}{\chi},z_j)\,, \quad (8)$$

which also allows a direct measurement of $R_{SN}(z)$, where $C_{\gamma G}$ is sensitive mainly to $z \lesssim 1$ because of the increased

density fluctuations and more easily observable galaxies at lower redshifts.

5. OBSERVATIONAL FEASIBILITY

The three methods discussed above to recover $R_{SN}(z)$ involve very few assumptions. The cosmological parameters have been or will be measured precisely, and measurements of galaxy clustering over a broad range of scales are also rapidly improving. The multiwavelength properties and possible evolution of SNIa will be calibrated by present and future observations. Thus the feasibility of our proposed methods depends mainly on the CGB observations. Low gamma ray fluxes and low S/N make the measurements of $\bar{F}(E)$, $C_{\gamma G}$, and especially C_γ highly challenging, but the results would provide new and important tests of $R_{SN}(z)$. Here we estimate the requirements for such measurements.

In the MeV range, the main noise sources arise from cosmic rays and radioactivities in the detectors (Weidenspointner 1999); these can be treated as Poisson noise and subtracted. Then the uncertainty in the measured C_γ is given by

$$\frac{\delta(C_\gamma \bar{F}^2)}{C_\gamma \bar{F}^2} = \sqrt{\frac{1+(1+\frac{C_{N,\gamma}}{W_\ell^2 C_\gamma})^2}{(2\ell+1)\Delta\ell f_{\rm sky}^{CGB}}}. \quad (9)$$

The noise power spectrum is given by $C_{N,\gamma} = 4\pi f_{\rm sky}^{CGB}[(N_{N,\gamma}/N_\gamma)^2/N_{N,\gamma} + 1/N_\gamma]$, where the first term is the Poisson noise of the instrumental background and the the second term is the Poisson noise of the signal. Here $f_{\rm sky}^{CGB}$ is the fractional sky coverage, and $N_{N,\gamma}$ and N_γ are the total numbers of received instrumental events and CGB gammas, respectively. Each SNIa contributes much less than one detected gamma ray, so the signal Poisson noise is determined by N_γ instead of the total number of SNIa in the survey volume and observing period. The window function W_ℓ reflects the angular resolution of CGB experiment, which we assume to be $W_\ell = \exp(-\ell^2\theta_p^2/16\sqrt{\pi})$, where θ_p is the angular resolution of the survey.

For fixed survey time (fixed $N_{N,\gamma}$ and N_γ), the optimal survey strategy has to compromise between a larger $f_{\rm sky}$, which decreases the cosmic variance, and a smaller $f_{\rm sky}$, which decreases the noise power spectrum $C_{N,\gamma}$. Thus there exists an optimal sky coverage $f_{\rm sky}^{\rm opt}$ for each ℓ such that the relative error of C_γ is the smallest:

$$f_{\rm sky}^{\rm opt} = \min\left(\frac{\sqrt{2}W_\ell^2 C_\gamma}{C_{N,\gamma}(f_{\rm sky}^{CGB}=1)}, 1\right). \quad (10)$$

The uncertainty in the measured $C_{\gamma,G}$ is then given by

$$\frac{\delta(C_{\gamma G}\bar{F}\bar{\Sigma}_G)}{C_{\gamma G}\bar{F}\bar{\Sigma}_G} = \sqrt{\frac{1+r^{-2}(1+\frac{C_{N,\gamma}}{W_\ell^2 C_\gamma})(1+\frac{C_{N,G}}{W_\ell^2 C_G})}{(2\ell+1)\Delta\ell\ \min(f_{\rm sky}^{CGB}, f_{\rm sky}^{G})}}. \quad (11)$$

The noise power spectrum of the galaxy survey is $C_{N,G} = 4\pi f_{\rm sky}^G/N_G$, where N_G is the number of galaxies observed with a sky coverage $f_{\rm sky}^G$, and r is the cross correlation coefficient between the CGB and a galaxy survey. For the cross correlation, larger $f_{\rm sky}^{CGB}$ always improves the measurement. Our results are shown in Fig. 3. We found

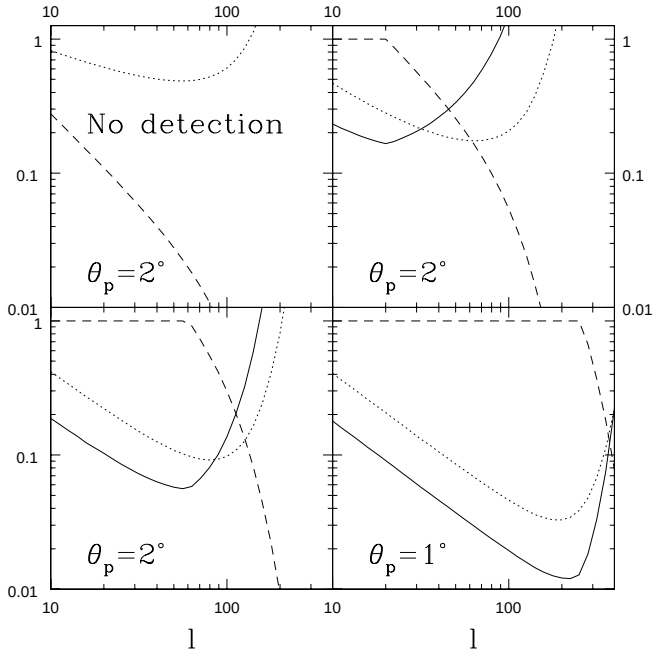

FIG. 3.— Estimated optimal sky coverage (dashed line) and corresponding optimal relative errors in C_γ (solid lines) and $C_{\gamma G}$ (dotted lines) measurements. We assume SDSS for the photometric galaxy survey, which will measure $N_G \sim 5\times10^7$ galaxies and cover a quarter of the sky. The SNIa CGB gamma flux is $\sim 10^7\,(100\ {\rm cm}^2)^{-1}\ {\rm sr}^{-1}\ {\rm yr}^{-1}$. Since the power spectra vary slowly with ℓ, we adopted a bin size $\Delta\ell = 0.3\ell$. Moving from left to right across the top row, and then again across the bottom row, the values of $(N_\gamma, N_\gamma/N_{N,\gamma})$ are: $(10^7, 0.01), (10^7, 0.1), (10^7, 1), (10^8, 1)$, respectively in rough correspondence to COMPTEL, MEGA or NCT, ACT, and a several-year ACT-like experiment with better angular resolution.

that the optimal angular scale for correlation detections is the degree scale, essentially the smallest scale allowed by the detector angular resolution. Though higher accuracy could be achieved at smaller scales, some of the assumptions about Gaussian fluctuations and constant bias may begin to break down.

The key requirements for the necessary detections are (a) good S/N ($\gtrsim 0.1$), (b) large sky coverage ($f_{\rm sky} \sim 1$), and (c) large number of gamma detections ($N_\gamma \sim 10^7$). The gamma flux is $\sim 10^7\ (100\ {\rm cm}^2)^{-1}\ {\rm sr}^{-1}\ {\rm yr}^{-1}$, so a field of view of ~ 1 sr and an integration time of ~ 1 year are required. These requirements guarantee $\sim 10^3$ contributing SNIa per pixel, and will average out the time dependence of the SNIa gamma ray emission (bright for ~ 1 year) and possible dispersion in SNIa spectra.

COMPTEL satisfied all of these requirements but (a). Its poor S/N makes the measurement of C_γ and $C_{\gamma G}$ unfeasible, as illustrated in Fig. 3. The proposed Advanced Compton Telescope (ACT) [1] satisfies all three requirements (Milne, Kroeger, Kurfess, & The 2002). With ACT and SDSS, several percent precision in both C_γ and $C_{\gamma G}$ measurement would be possible (Fig. 3), and this would allow a comparable precision in the inverted $R_{SN}(z)$. MEGA [2] (Bloser et al. 2002) and and NCT [3]

[1] ACT, http://hese.nrl.navy.mil/gamma/detector/ACT/ACT.htm
[2] http://www.mpe.mpg.de/gamma/instruments/mega/www/mega.html
[3] http://ssl.berkeley.edu/gamma/nct.html

fall in between COMPTEL and ACT. The ultimate possible precision, $\sim 1\%$, is set by the limited gamma flux in a one year survey.

6. DISCUSSION AND SUMMARY

We have presented the power of using angular correlations to identify and measure the SNIa component of the MeV CGB. The CGB fluctuations should follow from the underlying large-scale structure of galaxies on degree scales, with rms fluctuations varying from several $\sim 1\%$ to order unity, depending on the energy band. At the degree scale, such measurements are feasible and the interpretation is robust. We estimate that ACT + SDSS would be able to measure C_γ and $C_{\gamma G}$ with several percent accuracy. The combination of CGB mean flux and angular correlations will help to separate SNIa contributions from other possible sources and allows an statistically robust measurement of the SNIa rate to $z \sim 1$. Additionally, our proposed inversion technique using the mean flux spectrum would probe the SNIa and SFR rates to even higher redshifts.

A variety of new physics models predict or allow contributions to the present-day MeV CGB, for example the decay of non-baryonic cold dark matter (Olive & Silk 1985; Barbieri & Berezinsky 1988; Daly 1988; Gondolo 1992; Ellis et al. 1992; Kamionkowski 1994; Kribs & Rothstein 1997; Abazajian, Fuller, & Patel 2001; Chen & Kamionkowski 2003), the decay of massive gravitons predicted by models of extra dimensions (Arkani-Hamed, Dimopoulos, & Dvali 1999; Hall & Smith 1999; Hannestad & Raffelt 2003; Casse, Paul, Bertone, & Sigl 2003), and primordial black hole evaporation (Kim, Lee, & MacGibbon 1999; Daghigh & Kapusta 2002; Sendouda, Nagataki, & Sato 2003). When those photons arise from high-redshift sources, their angular distribution will be very isotropic and their energy spectrum may be featureless, though they may contribute an MeV CGB flux comparable to the observations. However, such sources may be separated from the SNIa contribution by using the techniques introduced in this paper, allowing more stringent tests of new physics than with the flux constraint alone. Similarly, these techniques can discriminate against exotic gamma ray sources that follow the halo profile of the Milky Way.

Finally, if the origin of the MeV cosmic *gamma ray* background is indeed type Ia supernovae, then this flux should be closely connected to the ~ 10 MeV cosmic *neutrino* background from type II, Ib, and Ic (core-collapse) supernovae. Type Ia supernovae (arising from stars less massive than about $8M_\odot$) only efficiently produce gamma rays, and core-collapse supernovae (arising from stars more massive than about $8M_\odot$) only efficiently produce neutrinos. Nevertheless, for an assumed initial mass function, the ratio of the gamma ray and neutrino fluxes should be mostly independent of the SFR.

Each type Ia supernova produces $\sim 0.5M_\odot$ of ^{56}Ni, leading to $\sim 10^{55}$ gamma rays. In contrast, in a core-collapse supernova, the inner $\sim 1.5M_\odot$ core radiates about $\sim 10^{58}$ neutrinos, the dominant energy loss mechanism. The core-collapse supernova rate is about 10 times larger than the type Ia supernova rate, so therefore the supernova neutrino background flux should exceed the supernova gamma ray background flux by $\sim 10^4$. Recently, the experimental limit on the supernova neutrino flux has been greatly improved by Malek et al. (2003), and is now very near the theoretical predictions (Kaplinghat, Steigman, & Walker 2000; Fukugita & Kawasaki 2003; Ando, Sato, & Totani 2003; Strigari, Kaplinghat, Steigman, & Walker 2003). In addition, Beacom & Vagins (2003) have shown that a modification of the Super-Kamiokande detector would dramatically improve the signal to noise, allowing a clear discovery.

Though neither the gamma ray nor neutrino background has been clearly measured yet, the predicted integrated fluxes, with $F_\nu \sim 10^2$ cm^{-2} s^{-1} (summed over flavors) and $F_\gamma \sim 10^{-2}$ cm^{-2} s^{-1}, are indeed in roughly the expected ratio. In the standard scenario, both backgrounds arise dominantly from supernovae with $z \lesssim 1$. Exotic scenarios might predict rather different flux ratios, or might produce gamma rays and neutrinos at high redshift, such that the gamma rays cascade to lower energies by scattering, but the neutrinos simply redshift. Though at present this comparison is rather crude, it could be made much more precise, and the excellent prospects for detection of both the gamma ray and neutrino backgrounds makes this potentially a very important test of the assumed astrophysical scenarios (e.g., the timescale for a binary to form a SNIa) as well as more exotic physics models.

Acknowledgments: We thank Brian Fields and Dieter Hartmann for helpful discussions. This work was supported by Fermilab (operated by URA under DOE contract DE-AC02-76CH03000) and by NASA grant NAG5-10842.

REFERENCES

Abazajian, K., Fuller, G. M., & Patel, M. 2001, Phys. Rev. D, 64, 023501
Ando, S., Sato, K., & Totani, T. 2003, Astroparticle Physics, 18, 307
Arkani-Hamed, N., Dimopoulos, S., & Dvali, G. 1999, Phys. Rev. D, 59, 086004
Barbieri, R.& Berezinsky, V. 1988, Physics Letters B, 205, 559
Beacom, J. F. & Vagins, M. R. 2003, hep-ph/0309300
Bloser, P. F., Andritschke, R., Kanbach, G., Schönfelder, V., Schopper, F., & Zoglauer, A. 2002, New Astronomy Review, 46, 611
Casse, M., Paul, J., Bertone, G., & Sigl, G. 2003, hep-ph/0309173
Blom, J. J. et al. 1995, A&A, 298, L33
Chen, X. & Kamionkowski, M. 2003, astro-ph/0310473
Clayton, D. D. & Silk, J. 1969, ApJ, 158, L43
Clayton, D. D. & Ward, R. A. 1975, ApJ, 198, 241
Cline, D. B. & Gao, Y. 1990, ApJ, 348, 33
Connolly, A. J. et al. 2002, ApJ, 579, 42
Daly, R. A. 1988, ApJ, 324, L47
Dodelson, S. et al. 2002, ApJ, 572, 140
Ellis, J., Gelmini, G. B., Lopez, J. L., Nanopoulos, D. V., & Sarkar, S. 1992, Nuclear Physics B, 373, 399
Fukugita, M. & Kawasaki, M. 2003, MNRAS, 340, L7
Gao, Y., Cline, D. B., & Stecker, F. W. 1990, ApJ, 357, L1
Gondolo, P. 1992, Physics Letters B, 295, 104
Hall, L. J. & Smith, D. 1999, Phys. Rev. D, 60, 085008
Hannestad, S. & Raffelt, G. G. 2003, Phys. Rev. D, 67, 125008
Hippelein, H. et al. 2003, A&A, 402, 65
Kamionkowski, M. 1994, astro-ph/9404079
Daghigh, R. & Kapusta, J. 2002, Phys. Rev. D, 65, 064028
Kaplinghat, M., Steigman, G., & Walker, T. P. 2000, Phys. Rev. D, 62, 043001

Kim, H. I., Lee, C. H., & MacGibbon, J. H. 1999, Phys. Rev. D, 59, 063004
Kribs, G. D. & Rothstein, I. Z. 1997, Phys. Rev. D, 55, 4435; *ibid* 56, 1822
Malek, M. et al. 2003, Physical Review Letters, 90, 061101
Milne, P. A., Kroeger, R. A., Kurfess, J. D., & The, L.-S. 2002, New Astronomy Review, 46, 617
Miniati, F. 2003, MNRAS, 342, 1009
Olive, K. A. & Silk, J. 1985, Physical Review Letters, 55, 2362
Peacock, J.A., 1999, *Cosmological Physics*, Cambridge University Press
Ruiz-Lapuente, P.; Cassé, M.; Vangioni-Flam, E., 2001, ApJ, 549, 483
Sendouda, Y., Nagataki, S., & Sato, K. 2003, Phys. Rev. D, 68, 103510
Strigari, L. E., Kaplinghat, M., Steigman, G., & Walker, T. P. 2003, astro-ph/0312346
The, L., Leising, M. D., & Clayton, D. D. 1993, ApJ, 403, 32
Timmes, F. X. & Woosley, S. E. 1997, ApJ, 489, 160
Watanabe, K., Hartmann, D. H., Leising, M. D., & The, L.-S. 1999, ApJ, 516, 285
Watanabe, K., Leising, M. D., Share, G. H., & Kinzer, R. L. 2000, American Institute of Physics Conference Series, 510, 471
Weidenspointner, G., 1999, Ph.D Thesis, Technische Univ. Munchen
Zhang, S. et al. 2002, A&A, 386, 843